

# Wake Integration to Predict Wing Span Loading from a Numerical Simulation

Donovan L. Mathias\*

*California Polytechnic State University,  
San Luis Obispo, California 93407*

James C. Ross†

*NASA Ames Research Center,  
Moffett Field, California 94035  
and*

Russell M. Cummings‡

*California Polytechnic State University,  
San Luis Obispo, California 93407*

## Introduction

**A**n important aspect in the application of computational fluid dynamics (CFD) is the determination of the resulting forces on the geometry of interest. The typical approach to computing forces on a body consists of integrating the pressures (and possibly skin friction) over the surface. However, the grid required to obtain an accurate resolution of the forces varies drastically with the geometry and can be memory-prohibitive in some cases. The integration of pressure can also provide some difficulties when overset grids are used due to the overlapping regions of the surface grids. A new approach to computing wing span loading from a CFD result is presented in this Note. The method uses the CFD solution to create an "equivalent" lifting line model from which the lift and induced drag are computed.

## Development of the Method

The current approach to computing a spanwise lift distribution is based on Prandtl's lifting line theory.<sup>1</sup> It is assumed that the lifting surface can be replaced by an infinite number of horseshoe vortices that extend infinitely far downstream. Implicit in the lifting line approach is the assumed validity of Helmholtz' vortex theorems,<sup>1</sup> which state the following:

1) A vortex filament maintains constant strength along its entire length.

2) A vortex filament can terminate at flow boundaries.

As a result of these theorems the circulation in the far wake can be related to the circulation along the lifting surface. The lift and induced drag can, therefore, be computed as long as the circulation in the wake is known. This approach directly relates the wake computed by a CFD flow solver to the circulation of the wing. A simple relationship is used, avoiding the need to compute the vorticity in the wake (since vorticity is computed using finite differences, it is very sensitive to the discretization), and avoiding the solution of Poisson's equation as in other approaches.<sup>2,3</sup>

Received Feb. 19, 1995; revision received March 20, 1995; accepted for publication March 27, 1995. Copyright © 1995 by the American Institute of Aeronautics and Astronautics, Inc. No copyright is asserted in the United States under Title 17, U.S. Code. The U.S. Government has a royalty-free license to exercise all rights under the copyright claimed herein for Governmental purposes. All other rights are reserved by the copyright owner.

\*Graduate Research Assistant; currently Graduate Research Assistant, Department of Aeronautics and Astronautics, Stanford University, Stanford, CA 94035. Student Member AIAA.

†Aerospace Engineer, Low Speed Aerodynamics Branch. Associate Fellow AIAA.

‡Department Chair and Professor, Aeronautical Engineering Department. Associate Fellow AIAA.

In viscous flow the strength of a vortex filament does not remain constant along its length due to viscous dissipation, and Helmholtz' vortex theorems are not strictly valid. In most CFD schemes things become even worse because additional dissipation is added to the flowfield either explicitly or implicitly through the computational mesh. For this reason, the circulation in the far wake cannot be equated to the circulation in the near field. Since this method uses wake integration to find the circulation distribution, the wake must be surveyed close to the body, before it is dissipated. In this way, an accurate circulation distribution can be computed from wake integration. The fact that Helmholtz' vortex theorems do not hold in the CFD solution does not reduce the validity of the approach since the CFD solution is only used to find the circulation as it is shed into the wake.

Lifting line theory states that the circulation shed in the wake of a lifting surface corresponds to the change in bound circulation (lift) along the surface. Therefore, the bound circulation at a point along the body can be found by integrating the wake circulation from a point outboard of the surface (where the lift and bound circulation are zero) to the point of interest on the surface. The following equation is used to perform the integration:

$$\Gamma = \oint_S \mathbf{v} \cdot d\mathbf{s}$$

where  $\Gamma$  is the circulation,  $S$  is the path of integration,  $d\mathbf{s}$  is the unit vector tangent to the path of integration, and  $\mathbf{v}$  is the local velocity vector.  $S$  must be defined so that the path encloses all of the shed circulation up to the point of interest.

A careful choice of  $S$  is required to obtain meaningful results using this method.  $S$  must form a continuous, closed path, but is not required to remain planar (i.e., perpendicular to the wake). However, the position of the intersection of the wake and the surface enclosed by  $S$  should lie very close to the aft end of the body. Also,  $S$  must extend beyond the body far enough to capture the circulation shed by the body portion of interest. The easiest way to ensure that the path does not affect the results is to begin with any path enclosing the wake and increase the area enclosed by the path until the circulation remains constant. Recomputing the circulation does not pose a significant computational penalty because each computation requires very little time.

There are a few considerations that need to be addressed when selecting an integration path. For example, the path should remain a few grid cells away from the grid outer boundaries. Depending on the boundary conditions specified, it is possible to develop an "artificial vorticity" buildup near the outer boundary. This occurs when freestream conditions are imposed on the grid outer boundary. If the circulation is computed using a path that consists entirely of outer boundary points, the result would be zero regardless of the proximity to a lifting body. However, the same path shifted inward a few grid cells will result in the correct circulation. This does not mean that the far-field circulation physically diminishes away from the body, but is artificially reduced by the boundary conditions. To eliminate any uncertainty associated with boundary conditions, the path should not be any closer to the outer boundary than necessary. In practice this is not a problem because the circulation is constant for most of the flowfield between the body and the outer boundaries. Extrapolated- and characteristic-type boundary conditions should not cause the same problems, but such types of boundary conditions have not been studied in this work.

All CFD results are sensitive to the computational mesh, and this method is no different. A mesh that is too coarse artificially dissipates the vorticity distributed throughout the grid. Thus, applying this method to a solution on a coarse mesh could result in circulation values that are too low. One

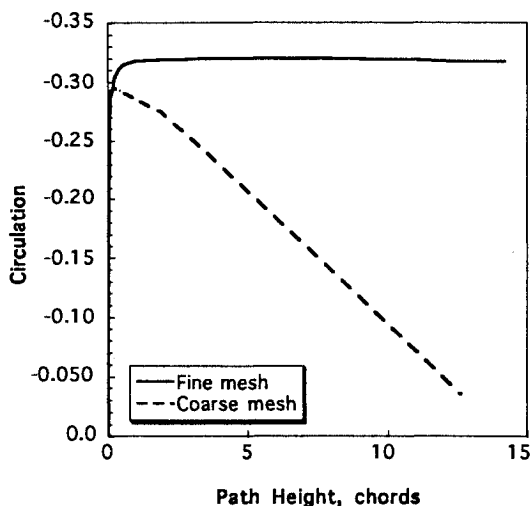


Fig. 1 Circulation vs integration path height.

indication of insufficient grid resolution is a circulation that does not become constant with increasing path height. For example, Fig. 1 shows the value of circulation at a fixed point along a wing plotted vs the height of the path above the wake for two grids. For the coarse grid, the circulation reaches its maximum value very close to the body and decreases rapidly with increasing path height. The circulation for the fine mesh, on the other hand, attains a value near the maximum very quickly and does not decrease.

To apply the method, the circulation is numerically evaluated along a path of connecting grid lines that comprise  $S$ . The velocities along the grid line, at points on each end of the segment, are averaged and multiplied by the length of the segment. These contributions to the total circulation are summed for each segment along  $S$ . Once  $\Gamma$  is known, the section lift coefficient can be computed from the following relation:

$$C_l = \frac{2\Gamma}{V_\infty c}$$

where  $V_\infty$  is the freestream velocity and  $c$  is the reference chord. The computation is then repeated for enough stations along the span to define the lift distribution.

The induced drag of the equivalent lifting line approximation can also be computed from the circulation distribution. The following equation is used<sup>4</sup>:

$$C_{D,i} = \frac{2}{V_\infty S} \int_{-b/2}^{b/2} \Gamma(y) \alpha_i(y) dy$$

where  $\alpha_i$  is the induced angle of attack given by

$$\alpha_i(y_0) = \frac{1}{4\pi V_\infty} \int_{-b/2}^{b/2} \frac{d\Gamma}{dy} \frac{dy}{y_0 - y}$$

This expression contains a singularity that can be numerically integrated if the singularity is excluded from the domain. Since the integrand has been discretized, all of the contributions to the integral can be summed, except when  $y_0$  is exactly  $y$ . For most meshes this approximation should prove adequate.

### Application of the Method

The current study applies this method to a simple, rectangular wing similar to the one experimentally investigated by Brune and Bogataj.<sup>2</sup> The wing had an AR of 6 with round

Table 1 Comparison of lift and induced drag coefficients

	Experiment	Computed	% Difference
$C_L$	0.566	0.551	2.5
$C_{D,i}$	0.017	0.016	4.5

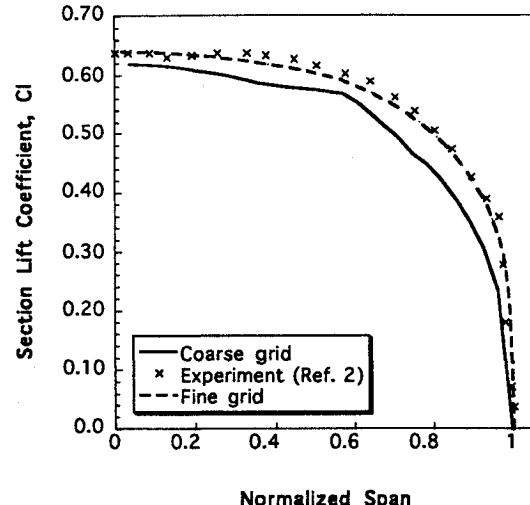


Fig. 2 Lift distribution comparison.

wingtips whose radius was determined by the local airfoil thickness (NACA 0016) and was tested at  $M_\infty = 0.18$ ,  $Re_\infty = 1.27 \times 10^6$ , and  $\alpha = 8$  deg. The flow over the wing was computed using the INS3D-UPS incompressible Navier-Stokes solver and the Baldwin-Barth turbulence model.<sup>6</sup> Two variations of a single zone C-H grid topology were used to study the implications of the mesh on the method. The mesh sizes were  $61 \times 61 \times 41$  (streamwise, spanwise, and normal) points for the coarse mesh, and  $81 \times 81 \times 81$  for the fine mesh. A symmetry plane boundary condition was applied to the grid plane at the midspan of the wing so that only half of the flowfield was computed in both cases. In all cases the solutions were considered converged when the divergence of velocity fell below 0.1.

Figure 2 shows the lift distribution computed using this method for both meshes compared to the experimental results. The overall shape and magnitude of the lift distribution was captured fairly well in both cases. For the coarse mesh the computational method underpredicted the lift slightly over the entire span, with the greatest difference occurring just inboard of the tip. The finer mesh was created by adding additional points to these regions. The additional grid points improve the comparison dramatically. Some disagreement is seen near the middle of the half-span, which was a region not specifically resolved by the fine mesh. These results imply that the remaining disagreement could be eliminated by adding additional grid points. Note that the size of the fine mesh (530,000 points) is not too large to be of practical use, requiring approximately 15 min to converge on a current supercomputer.

The integrated lift and induced drag coefficients computed from the fine mesh are shown in Table 1 along with their experimental counterparts.<sup>2</sup> Reference 2 provides values taken during three successive tests, and the values listed in Table 1 are averages of these three runs. The experimental results appear to be repeatable to within 0.2% for the lift coefficient and just over 1% for the drag.<sup>2</sup> The experimental and computed lift coefficients differ by less than 3%, whereas the induced drag coefficients disagree by just under 5%. An uncertainty analysis performed by the authors of Ref. 2 predicted a 3% experimental uncertainty in the induced drag measure-

ments. Overall, the computed results agree very well with the experimental data.

### Conclusions

A new method of computing the spanwise lift distribution and induced drag from a CFD solution was developed. An equivalent lifting line model is created by integrating the circulation in the wake and it is used for loads computation. The method was applied to a simple, rectangular wing configuration, and the difference in lift and induced drag coefficients between computation and experiment was less than 3 and 5%, respectively. Results indicate that this method offers a simple alternative to computing lift and induced drag by pressure integration.

### Acknowledgments

This work was funded by NASA Ames Research Center Cooperative agreement NCC 2-813. The authors wish to thank

Vernon Rossow of Ames Research Center and Ilan Kroo of Stanford University for their helpful ideas and suggestions.

### References

- <sup>1</sup>Prandtl, L., and Tietjens, O. G., *Applied Hydro- and Aeromechanics*, McGraw-Hill, New York, 1934, pp. 198–203.
- <sup>2</sup>Brune, G. W., and Bogataj, P. W., “Induced Drag of a Simple Wing from Wake Measurements,” Society of Automotive Engineers Paper 901934, Oct. 1990.
- <sup>3</sup>Brune, G. W., “Quantitative Low-Speed Wake Surveys,” *Journal of Aircraft*, Vol. 31, No. 2, 1994, pp. 249–255.
- <sup>4</sup>Anderson, J., *Fundamentals of Aerodynamics*, McGraw-Hill, New York, 1984, pp. 249–255.
- <sup>5</sup>Rogers, S. E., “Numerical Solution of the Incompressible Navier-Stokes Equations,” NASA TM 102199, Nov. 1990.
- <sup>6</sup>Baldwin, B. S., and Barth, T. J., “A One-Equation Turbulent Transport Model for High Reynolds Number Wall Bounded Flows,” AIAA Paper 91-0160, Jan. 1991.